

The role of the geothermal heat flux in driving the abyssal ocean circulation

A. Mashayek,¹ R. Ferrari,² G. Vettoretti,¹ and W. R. Peltier¹

Received 24 April 2013; revised 4 June 2013; accepted 5 June 2013; published 25 June 2013.

[1] The results presented in this paper demonstrate that the geothermal heat flux (GHF) from the solid Earth into the ocean plays a non-negligible role in determining both abyssal stratification and circulation strength. Based upon an ocean data set, we show that the map of upward heat flux at the ocean floor is consistent (within a factor of 2) with the ocean floor age-dependent map of GHF. The observed buoyancy flux above the ocean floor is consistent with previous suggestions that the GHF acts to erode the abyssal stratification and thereby enhances the strength of the abyssal circulation. Idealized numerical simulations are performed using a zonally averaged single-basin model which enables us to address the GHF impact as a function of the depth dependence of diapycnal diffusivity. We show that ignoring this vertical variation leads to an under-prediction of the influence of the GHF on the abyssal circulation. Independent of the diffusivity profile, introduction of the GHF in the model leads to steepening of the Southern Ocean isopycnals and to strengthening of the eddy-induced circulation and the Antarctic bottom water cell. The enhanced circulation ventilates the GHF derived heating to shallow depths, primarily in the Southern Ocean. **Citation:** Mashayek, A., R. Ferrari, G. Vettoretti, and W. R. Peltier (2013), The role of the geothermal heat flux in driving the abyssal ocean circulation, *Geophys. Res. Lett.*, *40*, 3144–3149, doi:10.1002/grl.50640.

1. Introduction

[2] It has been argued in the literature (*Emile-Geay and Madec* [2009]) that even though the geothermal heat flux (GHF) is approximately 1000× smaller than air-sea buoyancy flux, it may nevertheless play an important role in the ocean circulation since heating the oceans from below supports a more efficient closed Meridional Overturning Circulation (MOC). This basal heating acts to increase the Available Potential Energy of the ocean general circulation. Moreover, while air-sea fluxes are large, their strength and sign have strong latitudinal dependence, whereas the GHF is unidirectional. Furthermore, insofar as the Antarctic Bottom Water (AABW) circulation is concerned, air-sea fluxes are in contact with the cell over a surface area which is about 1000

times smaller than the contact area of the cell with the ocean floor, rendering the importance of the bottom and surface fluxes comparable.

[3] *Scott et al.* [2001] and *Adcroft et al.* [2001] investigated the influence of the GHF on the ocean circulation by means of coarse resolution ocean general circulation model (OGCM) simulations with a uniform heat flux of 50 mWm⁻² imposed over the ocean floor. Their main conclusions were that inclusion of the GHF leads to the erosion of the abyssal stratification, and that the heat transferred to the ocean from below is transported by the AABW circulation and is thereby ventilated to the surface of the Southern Ocean. They also showed that the strength of the AABW cell is inversely proportional to the abyssal stratification, a result that has been reinforced by the recent theoretical study of *Nikurashin and Vallis* [2011] (hereafter NV11). By comparing numerical simulations of ocean circulation with and without inclusion of the GHF, *Adcroft et al.* [2001] concluded that inclusion of the GHF increases the rate of abyssal circulation by approximately 25%. *Emile-Geay and Madec* [2009] later studied the same problem using an OGCM by considering the interplay between enhanced abyssal mixing and the GHF. They employed both a uniform flux of 87 mWm⁻² and a realistic spatially varying heat flux. They showed that the introduction of the GHF leads to erosion of the abyssal stratification and an enhancement of the abyssal circulation by about 15% for the case with uniform GHF and by a more modest amount once a realistic heat flux map is employed. They also found that the impact of the GHF on abyssal circulation is more pronounced in the Indo-Pacific Ocean compared to the Atlantic. They argued that this results from a relatively larger downward buoyancy flux which exists in the Atlantic Ocean due to the large density difference between the North Atlantic Deep Water and AABW cells. This large downward flux dominates the upward GHF, whereas in the Indo-Pacific basin, the downward flux is smaller, allowing the GHF to play a more important role, consistent with the findings of *Scott et al.* [2001]. *Hofmann and Maqueda* [2009] have revisited this problem and argued that GHF values in the range 50–87 mWm⁻² employed in earlier studies were too low, and that a mean flux of 100 mWm⁻² would be more reasonable and still conservative. By imposing this value in the OGCM, they obtained an increase in the AABW overturning rate of 33%.

[4] In what follows, we first employ an ocean data set to investigate whether the erosion of abyssal stratification is evident. We then perform a set of numerical simulations using a zonally averaged model to investigate the effect of GHF by considering a range of values from 0 to 75 mWm⁻². We will show that if the diapycnal diffusivity profile is vertically constant in the abyss, the strengthening of the abyssal

Additional supporting information may be found in the online version of this article.

¹Department of Physics, University of Toronto, Toronto, Ontario, Canada.

²Department of Earth, Atmospheric and Planetary Sciences, Massachusetts Institute of Technology, Cambridge, Massachusetts, USA.

Corresponding author: A. Mashayek, University of Toronto, 60 St. George Street, Room 609, Toronto, ON, M5S 1A7, Canada. (amashaye@atmosph.physics.utoronto.ca)

circulation due to the increase in the GHF is consistent with earlier studies. However, if the profile is enhanced sharply in the abyss consistent with the available observations, the influence of GHF is enhanced. This suggests that as more realistic parameterizations of abyssal mixing are employed, the influence of GHF may prove to be even more significant than previously suggested.

2. World Ocean Circulation Experiment Analysis

[5] To investigate the abyssal fluxes of heat and buoyancy, we present an analysis similar to *Emile-Geay and Madec* [2009] but considering the impact of vertically dependent diffusivity profiles inferred from observations. More specifically, we employ the World Ocean Circulation Experiment (WOCE) data set (*Gouretski and Koltermann* [2004]) along with the basin averaged profiles of diapycnal diffusivity for the Atlantic Ocean, the Indo-Pacific Ocean, and the Southern Ocean from *Lumpkin and Speer* [2004]. Since great uncertainty is associated with the diffusivity profiles, especially in our region of interest in the abyssal ocean, the results of our analyses will inherit the corresponding uncertainty. However, this uncertainty will not undermine our main conclusions.

[6] Figure 1(top) shows the heat flux, computed as the vertical temperature gradient times the diffusivity, at the base of the ocean and the middle two panels of the figure show zonally averaged maps of the heat flux in the Atlantic and Indo-Pacific basins (details of the calculations are provided in the supporting information). The top panel in the figure has a pattern similar to maps of the geothermal heat flux (such as those provided in *Emile-Geay and Madec* [2009] and *Davies and Davies* [2010]) since mid-ocean ridges are regions of enhanced mixing as well as large GHF. The bottom panel in Figure 1 shows the geothermal heat flux inferred from the age of the seafloor averaged over various ocean basins (calculated from the GHF data set of *Emile-Geay and Madec* [2009]). Henceforth, we will focus on zonally averaged heat fluxes in the Atlantic and Indo-Pacific basins and will not further discuss results for the zonally averaged Southern Ocean for two reasons: the diffusivity profiles are far too uncertain in the Southern Ocean to yield acceptable estimates and the theoretical model which we employ to perform idealized simulations does not allow us to study the role of GHF in the Southern Ocean dynamics adequately. The zonally averaged map of the heat flux in the Atlantic Ocean shows that the downward diffusive flux dominates the basin to a depth of 5000 m. The Indo-Pacific Ocean plot, on the other hand, shows a balance between the downward diffusion of heat from the surface and the upward GHF at depths below 4500 m. Comparison between the heat flux contour levels above the ocean floor in the two middle panels with the zonally-averaged GHF curves in the bottom panel shows that the GHF is of leading order in both the Atlantic and the Indo-Pacific basins. However, in the Indo-Pacific basin, the influence of GHF seems to be larger, perhaps because of the larger averaged fluxes in the Indo-Pacific (due to large GHFs at the East Pacific rise) as well as the more pronounced downward diffusive flux in the Atlantic which exists because of the presence of the significant temperature difference between the two Atlantic overturning cells.

3. Idealized Simulations

[7] A number of idealized simulations have been performed to investigate the role of the GHF on the abyssal stratification and circulation. For this purpose, we have closely followed the theoretical formulation of the zonally-averaged numerical model of NV11, the sole exception being that we will allow for vertical variation in the diapycnal diffusivity. Figure 2(top) provides a schematic of the numerical model. Details of the numerical model and its implementation as well as the relevant boundary conditions are described in the supporting information. In short, the computational domain in the model consists of a zonally periodic channel (representative of the Southern Ocean) attached to a zonally-averaged ocean basin to the north. For the periodic channel, we solve the following equations:

$$\Psi = \Psi_w + \Psi_{\text{eddy}} = \frac{\tau}{f\rho_0} + K_e s_b, \quad (1)$$

$$b_t + \bar{b}_z \Psi_y - \bar{b}_y \Psi_z = \partial_z(\kappa \bar{b}_z), \quad (2)$$

which represent the momentum budget and an advection-diffusion equation for buoyancy, respectively, and where τ is the surface wind stress, f is the Coriolis parameter, K_e is the isopycnal eddy diffusivity, s_b represents the isopycnal slopes, and b is buoyancy ($b = -g(\rho - \rho_0)/\rho_0$ and ρ is density). Equation (1) shows that the circulation in the Southern Ocean is controlled by a clockwise Eulerian mean wind circulation and a counterclockwise eddy circulation which represents the slumping of isopycnals as a result of baroclinic instabilities. The left-hand side of equation (2) represents the along-isopycnal transport by the residual circulation and the right-hand side represents the diapycnal mixing. In the zonally-averaged ocean basin, we solve a simplified advection-diffusion equation of the form

$$b_t + \bar{b}_z \Psi_y = \partial_z(\kappa \bar{b}_z), \quad (3)$$

in which it is assumed that $s_b \approx 0$ (motivated by observations).

[8] Equations (1–3), along with proper boundary conditions (see supporting information), describe the overturning circulation in the channel and in the ocean basin and can be integrated in time to solve for the evolution of the buoyancy field and from that for the evolution of the circulation. At each time step, it is ensured that both the buoyancy and total streamfunction in the channel match those of the basin at their interface. For all the cases to be discussed below, the equations have been integrated in time until the flow has reached a steady-state solution, i.e., when changes in the streamfunction at the channel-basin interface are smaller than 0.1%. Thus, time dependence will be neglected in the analyses to follow.

[9] The basin component of the circulation represented by equation (3) will be the focus of our analyses in this section. By expanding the term $(\kappa b_z)_z$, this equation implies that the strength of the circulation depends on a balance between two terms with opposing influences: namely the κb_{zz} term, which is positive in the deep ocean and which promotes an anti-clockwise circulation (same sense as the eddy circulation in the Southern Ocean) and the $\kappa_z b_z$ term which is negative and which promotes a clockwise circulation (same sense as that forced by the wind stress over the Southern Ocean). Therefore, the vertical decay in the intensity of the

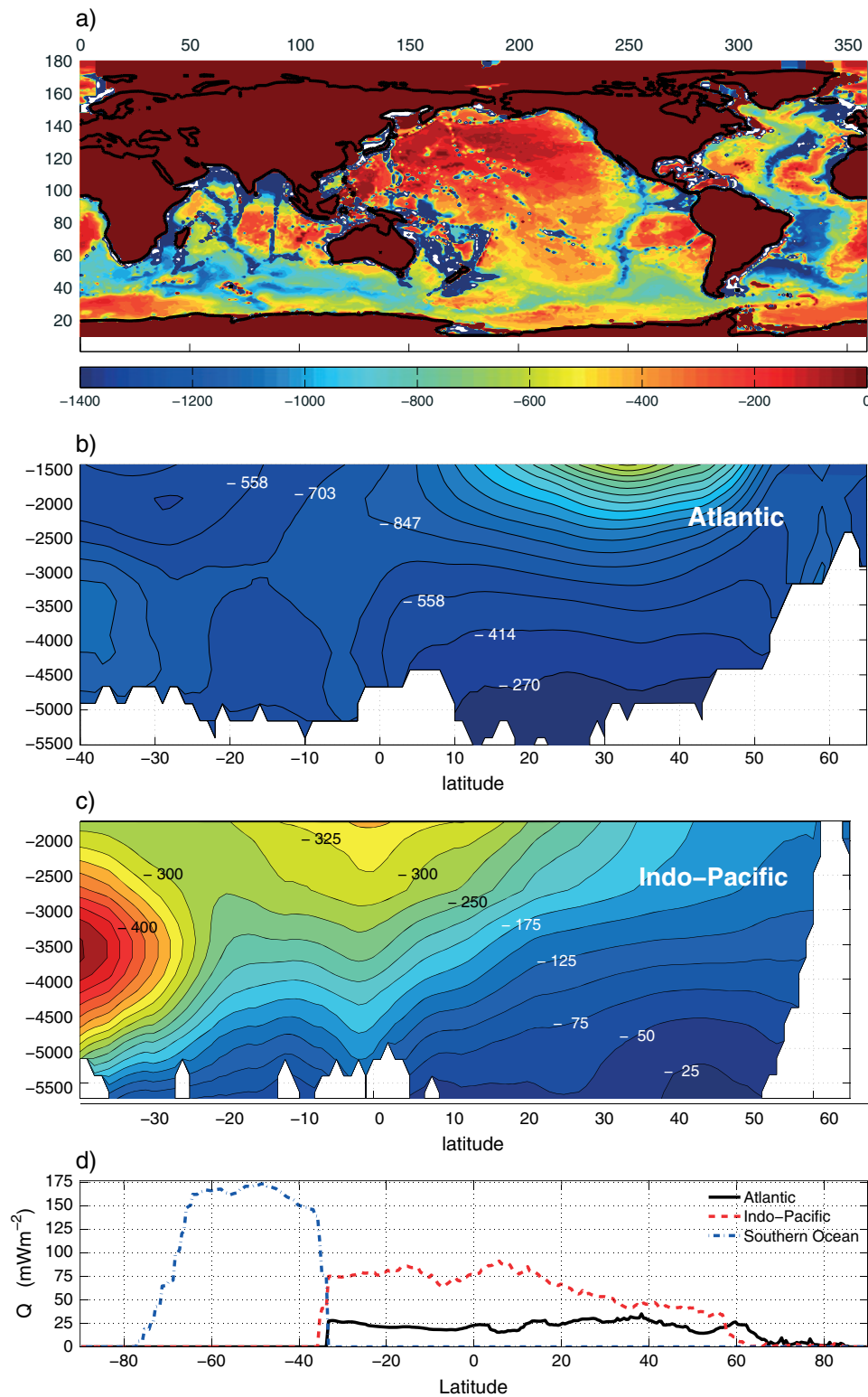


Figure 1. Map of the downward heat flux at the bottom of the ocean calculated from the WOCE data set (first panel); zonally averaged diffusive heat flux $\rho_0 C_p k T_z$ in the Atlantic and Indo-Pacific basins (second and third panels); geothermal heat flux inferred from the age of the seafloor averaged over various ocean basins (fourth panel) (calculated from analyses of *Emile-Geay and Madec* [2009]). Contour levels in the second and third panels are in mWm⁻². Details of the calculations are described in the supporting information.

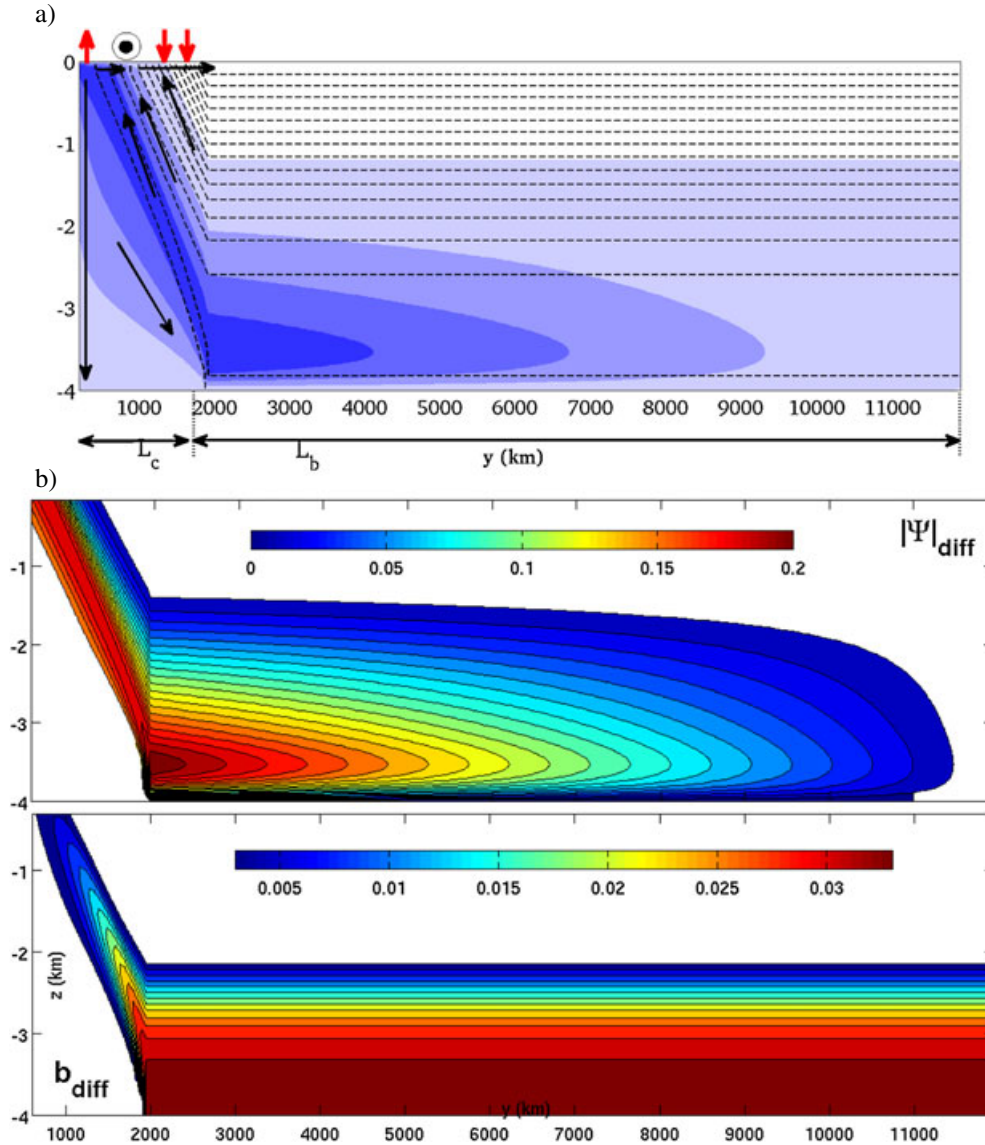


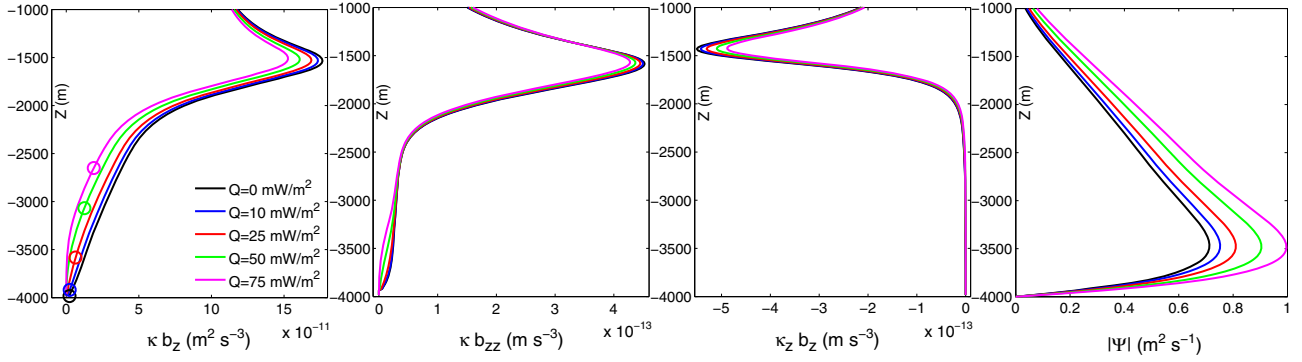
Figure 2. (top) Schematic of the zonally averaged model (see supporting information for detailed description); Difference maps for (middle) streamfunction and (bottom) buoyancy constructed by subtracting the fields associated with the control run (with no basal heating) from a case with uniform GHF of 50 mWm^{-2} (both cases with the exponential diffusivity profile). Middle panel is in units of $\text{m}^2 \text{ s}^{-1}$ while the contour levels in the bottom panel is normalized by Δb , the buoyancy difference across the Southern Ocean channel at the surface of the ocean (set to 0.02 m s^{-2} in the simulations).

abyssal turbulent mixing suppresses the AABW circulation. To investigate the influence of these two terms on the abyssal stratification and buoyancy flux, we consider two sets of simulations, one based upon the assumption of an exponential κ profile (with a vertical scale of $H = 500 \text{ m}$) and the other based upon the use of a Bryan and Lewis profile (hereafter referred to as the BL79 profile which is due to *Bryan and Lewis* [1979]; see Figure S2 for profile equations). Both profiles have values of $\kappa_b = 10^{-4} \text{ m}^2 \text{ s}^{-1}$ and $\kappa_t = 5 \times 10^{-6} \text{ m}^2 \text{ s}^{-1}$ at the ocean floor and at the base of the mixed layer, respectively. The exponential profile is characterized by a sharp vertical gradient associated with vertical decay of enhanced abyssal mixing. Such sharp variations have been demonstrated to be characteristic of the abyssal oceans through the application of inverse techniques by *Lumpkin and Speer* [2004], *Ganachaud and Wunsch*

[2000], and *Decloedt and Luther* [2012]. By comparing the results obtained using the two different diffusivity profiles, we will be able to assess the role of the suppressive term (i.e., $\kappa_b b_z$) on the right-hand side of (3) in the presence of the GHF. Motivated by the zonally averaged basal heat fluxes in the Atlantic and Indo-Pacific basins as plotted in Figure 1 (bottom), we consider various cases with uniform geothermal heat fluxes in the range $0 - 75 \text{ mWm}^{-2}$ as the bottom boundary condition of the computational domain.

[10] Figure 3 presents the results of the simulations for various GHF levels and for the two sets of experiments. The top row represents the BL79 diffusivity profile cases, while the bottom row shows those for the exponential diffusivity profile cases. The first panel in each row represents the vertical diffusive buoyancy flux, κb_z . For both diffusivity profiles, imposition of a nonzero GHF leads to the erosion of

BL79 diffusivity profile based results



exponential diffusivity profile based results

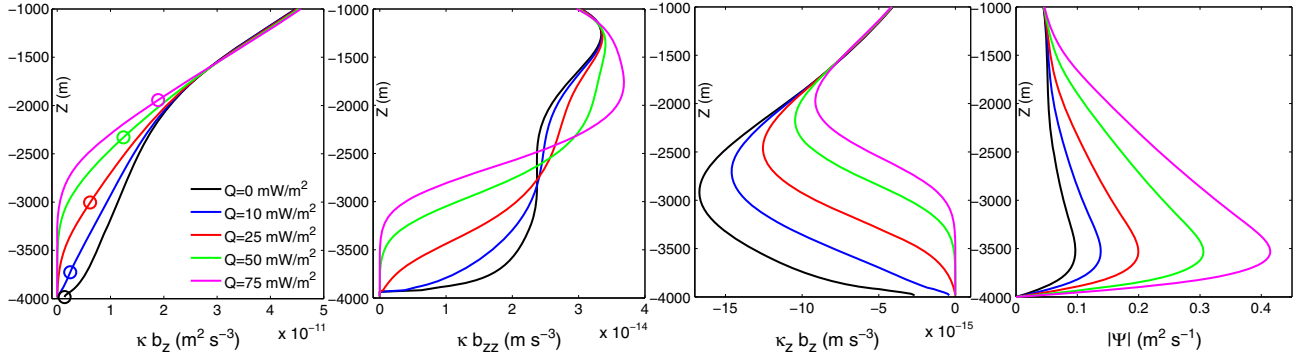


Figure 3. Profiles of κb_z , κb_{zz} , $\kappa_z b_z$, and $|\Psi|$ for various values of uniform GHF imposed at the bottom boundary. Top row shows results for simulations performed by using the *Bryan and Lewis* [1979] diffusivity profile and the bottom row shows similar results but for an exponential with a vertical length scale of 500 m. Line attributes in all panels are the same as left panels. The circles on each of the lines in the κb_z plots denote the depth at which the downward diffusive buoyancy flux matches the magnitude of the effective upward basal geothermal flux. Note that a heat flux of 50 mWm^{-2} corresponds to $\kappa b_z = 1.25 \times 10^{-11} \text{ m}^2 \text{ s}^{-3}$ due to $Q = -\frac{\rho_0 c_p}{g\alpha} (\kappa b_z)$, where α is the coefficient of thermal expansion of seawater ($\alpha \sim 10^{-4} \text{ K}^{-1}$).

the abyssal stratification, leaving an unstratified layer above the ocean floor. The thickness of this layer increases with increase in the geothermal flux for both diffusivity profiles but is considerably larger for the diffusivity profile with sharp variations. This is expected since $T_z \propto \text{GHF}/\kappa$ and since the diffusivity averaged over the abyssal depths is smaller for the exponential profile, the sensitivity of abyssal stratification to GHF is larger for the exponential profile. The small circle on each of the lines of the plot marks the depth at which the downward buoyancy flux is equal in magnitude (and opposite in direction) to the basal heat flux. Their position in elevation demonstrates that even conservative estimates of the basal heat flux match the downward buoyancy flux at mid-depths in the ocean. For sharp vertical variations of abyssal mixing (bottom row), basal heat flux matches the downward flux at even shallower depths as low as 1500–2000 m for $Q = 75 \text{ mWm}^{-2}$.

[11] The middle two panels in each of the two rows of Figure 3 show κb_{zz} and $\kappa_z b_z$. Both of these terms appear in the basin component of equation (1). As mentioned earlier, and as shown in the plots, the two terms are of opposite sign, with the former enforcing an anti-clockwise AABW circulation, and the latter suppressing it. Focusing on the top row and the BL79 profile, $\kappa_z b_z$ is negligible and κb_{zz} is characterized by small variations below the depth of 2000 m due to insignificant vertical variation in κ . In this case,

from equation (3), we get $|\Psi| \propto \kappa b_{zz}/b_z$. Both b_z and b_{zz} decrease in the abyss with increase in the GHF; however, the former decreases faster leading to an effective increase in the circulation as shown in the rightmost panel in the top row of the figure. We will discuss the physical reason for this increase in the context of our discussion of the bottom two panels of Figure 2. As compared to a case with no GHF, the circulation (measured at the depth of its maximum) increases by 27% for a GHF of 50 mWm^{-2} and by $\sim 39\%$ for a GHF of 75 mWm^{-2} , in qualitative agreement with earlier studies cited in the introduction. Focusing on the bottom row of Figure 3 and the results based on the exponential diffusivity profile, the $\kappa_z b_z$ term is no longer negligible, and in fact is comparable in magnitude to κb_{zz} (both $\mathcal{O}(10^{-14}) \text{ ms}^{-3}$). Therefore, the circulation in equation (3) is set by a balance between $\kappa_z b_z$ and κb_{zz} . Although an increase in the GHF leads to an increase in the abyssal circulation due to an effective increase in b_{zz}/b_z (similar to the BL79 cases), it also weakens the suppressing influence of $\kappa_z b_z$ by eroding the abyssal stratification. Therefore, an increase in the GHF leads to a more significant increase in the abyssal circulation when a sharp vertical variation of abyssal mixing is considered. As the last panel in the bottom row of Figure 3 demonstrates, the introduction of a GHF of $\sim 50\text{--}75 \text{ mWm}^{-2}$ leads to an increase of $\sim 200\text{--}300\%$ in the peak circulation.

[12] To discuss the physical reason behind the increase in overturning strength with increase in the GHF, we note that the slope of the isopycnals in the southern ocean can be estimated by $s_b = -b_y/b_z$ where b_y is the horizontal stratification. Since the basin and channel streamfunctions in equations (1–3) have to agree at the channel-basin boundary, a decrease in the abyssal stratification (i.e., decrease in b_z) in the basin due to the introduction of a GHF leads to an effective steepening (i.e., increase in s_b) of those Southern Ocean isopycnals which connect to the basin part of the AABW cell. Therefore, according to equation (1), this leads to an increase in the eddy-induced circulation for the same wind-driven circulation in the Southern Ocean and thereby to strengthening of the resulting AABW circulation. The middle panel of Figure 2 illustrates the increase in the anti-clockwise abyssal circulation (due to increase in eddy circulation in the Southern Ocean) induced by introducing a mean GHF of 50 mWm^{-2} . The bottom panel of the figure shows the corresponding effective increase in the buoyancy. The buoyancy injected into the ocean basin by the GHF finds its way to the ocean surface primarily in the Southern Ocean and by means of the increase in the eddy circulation associated with the Southern Ocean branch of the AABW cell (middle panel). Due to the simplifying assumptions made in our idealized model, the significant increase in the circulation shown in the rightmost panel of Figure 3 (for the cases with an exponential diffusivity profile) is not expected to provide a quantitative measure of the role of the GHF in the oceans. However, it very effectively illustrates the significant dependence of the influence of the GHF on the vertical variation of diapycnal mixing.

[13] Although our entire discussion has focused upon the modern circulation, we suspect that the influence of the GHF may be of even more significance to understanding climates of the distant past. For example, in the Neoproterozoic era of Earth history, it has been suggested that the planet may have become entirely glaciated with thick sea and land ice. Recent calculations of the bifurcation point in atmospheric carbon dioxide-solar luminosity space beyond which such states would be expected to form have cast significant doubt upon the plausibility of such snowball Earth occurrences (Hyde et al. [2000]; Peltier et al. [2004]; Yang et al. [2012]). Recently, Ashkenazy et al. [2013] suggested that the GHF could be crucial in driving a strong MOC during Snowball climates, but their analysis ignored the importance of sharp vertical variations in abyssal mixing.

4. Conclusions

[14] By employing an ocean data set and extending analyses of Emile-Geay and Madec [2009], we have shown that the vertical heat flux above the ocean floor under modern climate conditions is of the same order of and has a pattern similar to the estimates for the GHF induced by cooling of Earth's oceanic lithosphere. Results obtained using an idealized model are also in agreement with earlier studies in demonstrating that an increase in the rate of abyssal overturning arises as a consequence of the erosion of abyssal stratification by the GHF. This erosion was demonstrated to lead to steepening of the Southern Ocean isopycnals which connect to the AABW cell, leading to an increase in the eddy-induced transport and thereby to an increase in the strength of the abyssal circulation. It was shown that the

extent of influence of the heat flux depends heavily on the vertical dependence of the abyssal diapycnal mixing: sharp decay of the diffusivity profile in the abyss intensifies the influence of the geothermal flux and plays a primary role in setting the abyssal stratification and circulation.

[15] We emphasize that while the diffusivity profiles employed herein were useful in investigating the role of GHF in the presence of a strong vertical decay of diapycnal mixing immediately above the ocean floor at a constant depth of 4 km, mid-ocean ridges reach up to 2000 m elevation above the sea floor in the real ocean and thus the bottom topography may also significantly influence the sensitivity of the overturning circulation to the GHF. Therefore, we conclude by noting that an accurate quantitative estimation of the influence of GHF will require application of global models with appropriate representations of the bottom boundary layer, an accurate map of basal heat flux, and a high quality representation of diapycnal mixing throughout the abyssal ocean.

[16] **Acknowledgments.** This collaborative work was initiated and partly supported by a CNC/SCOR CMOS NSERC supplement as well as a CGCS fellowship to AM. We wish to thank M. Nikurashin and G. Stuhne for their help with implementation of the numerical model and J. Emile-Geay for providing the geothermal heat flux data used in Figure 1. The research of WRP is supported by NSERC Discovery Grant A9627 and research of RF is supported by NSF/OCE-1024198 grant.

[17] The Editor thanks one anonymous reviewer for his/her assistance in evaluating this paper.

References

- Adcroft, A., J. R. Scott, and J. Marotzke (2001), Impact of geothermal heating on the global ocean circulation, *Geophys. Res. Lett.*, **28**, 1,735–1,738.
- Ashkenazy, Y., H. Gildor, M. Losch, F. A. Macdonald, D. P. Schrag, and E. Tziperman (2013), Dynamics of a Snowball Earth ocean, *Nature*, **495**(7439), 90–93.
- Bryan, K., and L. J. Lewis (1979), A water mass model of the world ocean, *J. Geophys. Res.*, **84**, 2503–2517.
- Decloedt, T., and D. S. Luther (2012), Spatially heterogeneous diapycnal mixing in the abyssal ocean: A comparison of two parameterizations to observations, *J. Geophys. Res.*, **117**, C11025, doi:10.1029/2012JC008304.
- Emile-Geay, J., and G. Madec (2009), Geothermal heating, diapycnal mixing and the abyssal circulation, *Ocean Sci.*, **5**, 203–218.
- Davies, J. H., and D. R. Davies (2010), Earth's surface heat flux, *Solid Earth*, **1**, 5–24.
- Ganachaud, A., and C. Wunsch (2000), Improved estimates of global ocean circulation, heat transport and mixing from hydrographic data, *Nature*, **408**, 453–457.
- Gouretski, V., and K. P. Koltermann (2004), WOCE global hydrographic climatology, *Berichte des BSH*, **35**, 1–52.
- Hofmann, M., and M. A. M. Maqueda (2009), Geothermal heat flux and its influence on the oceanic abyssal circulation and radiocarbon distribution, *Geophys. Res. Lett.*, **36**, L03603, doi:10.1029/2008GL036078.
- Hyde, W. T., T. J. Crowley, S. Baum, and W. R. Peltier (2000), Neoproterozoic 'snowball Earth' simulations with a coupled climate/ice-sheet model, *Nature*, **405**, 425–429.
- Lumpkin, R., and K. Speer (2004), Global ocean meridional overturning, *J. Phys. Oceanogr.*, **37**, 2550–2562.
- Nikurashin, M., and G. Vallis (2011), A theory of deep stratification and overturning circulation in the ocean, *J. Phys. Oceanogr.*, **41**, 485–502.
- Peltier, W. R., L. Tarasov, G. Vettoretti, and L. P. Solheim (2004), Climate dynamics in deep time: Modeling the "snowball bifurcation" and assessing the plausibility of its occurrence, in *Neoproterozoic Glacial Extremes*, *Geophys. Monogr. Ser.*, vol. 146, edited by G. Jenkins et al., pp. 107–124, AGU, Washington, D. C.
- Scott, J. R., J. Marotzke, and A. Adcroft (2001), Geothermal heating and its influence on the meridional overturning circulation, *J. Geophys. Res.*, **106**(C12), 31,141–31,154.
- Yang, J., W. R. Peltier, and Y. Hu (2012), The initiation of modern "Soft Snowball" and "Hard Snowball" climates in CCSM3. Part II: Climate dynamic feedbacks, *J. Clim.*, **25**(8), 2737–2754.